

Strong shaking in Los Angeles expected from southern San Andreas earthquake

K. B. Olsen,¹ S. M. Day,¹ J. B. Minster,² Y. Cui,³ A. Chourasia,³ M. Faerman,³ R. Moore,³ P. Maechling,⁴ and T. Jordan⁴

Received 12 December 2005; revised 22 February 2006; accepted 27 February 2006; published 5 April 2006.

[1] The southernmost San Andreas fault has a high probability of rupturing in a large (greater than magnitude 7.5) earthquake sometime during the next few decades. New simulations show that the chain of sedimentary basins between San Bernardino and downtown Los Angeles form an effective waveguide that channels Love waves along the southern edge of the San Bernardino and San Gabriel Mountains. Earthquake scenarios with northward rupture, in which the guided wave is efficiently excited, produce unusually high long-period ground motions over much of the greater Los Angeles region, including intense, localized amplitude modulations arising from variations in waveguide cross-section. **Citation:** Olsen, K. B., S. M. Day, J. B. Minster, Y. Cui, A. Chourasia, M. Faerman, R. Moore, P. Maechling, and T. Jordan (2006), Strong shaking in Los Angeles expected from southern San Andreas earthquake, *Geophys. Res. Lett.*, *33*, L07305, doi:10.1029/2005GL025472.

[2] The right-lateral, strike-slip San Andreas Fault has produced a history of large (\sim M8) earthquakes [Sieh, 1978] most recently the 1906 event [Bolt, 1968] with tremendous damage to San Francisco. South of the 1906 rupture, the 1857 (El Cajon) earthquake ruptured the 360 km long stretch from Parkfield to Wrightwood [Weldon *et al.*, 2004]. However, the two segments of the San Andreas fault south of the 1857 rupture, the San Bernardino Mountains segment and the Coachella Valley segment, have not seen a major event since 1812 and about 1690 [Weldon *et al.*, 2004], respectively. The average recurrence interval for large earthquakes with surface rupture on these segments are $146 + 91 - 60$ yrs and 220 ± 13 yrs, respectively [Working Group on California Earthquake Probabilities, 1995]. A major component of the seismic hazard in southern California and northern Mexico comes from a large earthquake on this part of the San Andreas Fault [Frankel *et al.*, 2002]. Since no strike-slip earthquake of similar or larger magnitude has occurred since the first deployment of strong motion instruments in southern California, there is a large uncertainty of the ground motions expected from such event.

[3] To reduce this uncertainty we have carried out some of the largest and most detailed earthquake simulations completed to date (TeraShake), in which we model ground motions expected from a large earthquake on the southern San Andreas fault. Because these new simulations combine high spatial resolution with very large geographical extent, they reveal unexpected interactions between rupture directivity and shallow crustal structure. The TeraShake calculations simulate 4 minutes of 0–0.5 Hz ground motion in a 180,000 km² area of southern California, for a M 7.7 earthquake along the 200 km section of the San Andreas fault between Cajon Creek and Bombay Beach at the Salton Sea. The magnitude of the TeraShake scenarios was based on a conservative estimate of about 16 mm/yr for the average slip rate on the southern San Andreas fault [Sieh and Williams, 1990], accumulating a slip deficit of about 5 m since the last major event on this part of the fault.

[4] A decade ago, early studies estimated ground motions from a large earthquake on the San Andreas fault, roughly corresponding to the 1812 rupture from Tejon Pass to San Bernardino [Olsen *et al.*, 1995; Graves, 1998]. These simulations showed the importance of including a finite-source rupture model and a 3D earth structure accounting for realistic variations in seismic velocities, densities, and attenuation as well as 3D seismic wave propagation. Since these early studies, earth structure models [Magistrale *et al.*, 2000; Süss and Shaw, 2003] have improved considerably, and the profound effect of sedimentary basins, such as amplifying the seismic waves, prolonging their duration, and generating waves at the basin edges, have been documented in many areas [e.g., Olsen *et al.*, 2003; Pitarka *et al.*, 1998].

[5] The geographical area for the TeraShake simulations was a rectangular region, 600 km along N50°W and 300 km along N40°E, spanning southern California from the Ventura Basin, Tehachapi, and the southern San Joaquin Valley in the north, to Los Angeles, San Diego, and down to the Mexican cities of Mexicali, Tijuana, and Ensenada in the south (see Figure 1). The simulations used a 3,000 by 1,500 by 400 mesh, dividing the volume into 1.8 billion cubes with a spatial resolution of 200 meters. The 3-D crustal structure (Figure 2) was based on the SCEC Community Velocity Model (CVM) [Magistrale *et al.*, 2000; Kohler *et al.*, 2003] Version 3.0, with elastic parameters constrained by a large selection of data, including gravity, reflection seismics, oil-company drill-holes, and shallow geotechnical borings. The model extends to a depth of 80 km, including topography on the crust-mantle boundary and upper-mantle velocity variations [Kohler *et al.*, 2003]. The largest uncertainty in the CVM is located near the US-Mexican border, specifically the southern extension of the Salton Trough.

¹Department of Geological Sciences, San Diego State University, San Diego, California, USA.

²Scripps Institution of Oceanography, University of California, San Diego, La Jolla, California, USA.

³San Diego Supercomputer Center, University of California, San Diego, La Jolla, California, USA.

⁴Department of Earth Sciences, University of Southern California, Los Angeles, California, USA.



Figure 1. Location map for the TeraShake simulations. The red rectangle (121W, 34.5N; 118.9511292W, 36.621696N; 116.032285W, 31.082920N; 113.943965W, 33.122341N) depicts the simulation area, rotated 40° clockwise from North. The black rectangle depicts a section of the Los Angeles basin used for peak ground motion display. The dotted line depicts the part of the San Andreas Fault that ruptured in the TeraShake simulations. The N40°E dashed line depicts the location of the cross section used to approximate the crustal structure 50 km along N130°E until the southeastern border of the model.

Here, we approximated the crustal structure by repeating a N40°E trending cross section intersecting Mexicali (see Figure 1) 50 km along N130E° until the southeastern border of the model. The velocity of the near-surface layers was truncated at 500 m/s [Olsen *et al.*, 2003], an approximation which along with the selected grid spacing allows the resolution of the dominant phases propagating in the TeraShake model. Surface topography was neglected in order to preserve the numerical efficiencies of a Cartesian grid geometry.

[6] The San Andreas fault geometry was approximated as five vertical, planar segments from the 2002 USGS National Hazard Maps (Figure 1). The rupture length is 200 km, and the down-dip width is 15 km. The source model is based on that inferred for the 2002 Denali Earthquake (M7.9, the only instrumentally-recorded strike-slip earthquake in North America with magnitude similar to the TeraShake scenarios), from inversion of GPS and 0.01–0.5 Hz near-source seismic observations [Oglesby *et al.*, 2004]. Some modifications were made to the Denali model in order to transport it to the southern San Andreas (i.e., to bring it into conformance with the geometry and seismic moment of the TeraShake scenario), including neglecting the small dip-slip component of slip and adjusting the moment.

[7] Since it is uncertain where the next large event may nucleate on the southern San Andreas fault, the TeraShake simulations include scenarios with rupture initiating at either end of the fault. Three TeraShake simulations were carried out, all using a hypocentral depth of 10 km. One scenario starts at the northwestern end (34.29°N, 117.50°W) rupturing toward the southeast (NW-SE), and two start at

the southeastern end (33.35°N, 115.71°W) and rupturing toward the northwest (SE-NW1 and SE-NW2). The spatial and temporal slip distributions are the same for scenarios NW-SE and SE-NW1 (see Figure 2), while those for SE-NW2 are lateral mirror images of those from NW-SE and SE-NW1.

[8] Figure 3 shows the maximum root-mean-square (RMS) peak ground velocity (PGV) for all components inside portions of the modeling area for the NW-SE and SE-NW1 scenarios, with N50°W seismograms superimposed at selected sites. The PGV distributions reveal a striking contrast in ground motion pattern between NW-SE versus SE-NW rupture scenarios. The focusing of ground motion in the direction of rupture has been noted in previous simulations of long strike slip ruptures [Olsen *et al.*, 1995; Pitarka *et al.*, 1998], so the generally higher amplitudes to the north of the rupture from the SE-NW scenarios (relative to those from the NW-SE scenario) were expected. However, the simulations show that this rupture directivity effect is dramatically modified by interactions with the chain of sedimentary basins (the San Bernardino, Chino, San Gabriel, and Los Angeles basins) running westward from the northern terminus of the rupture to downtown Los Angeles (see crustal structure in Figure 2). This chain of basins forms a low-velocity structure that acts as a waveguide, trapping seismic energy along the southern edge of the San Bernardino and San Gabriel Mountains and channeling it into the Los Angeles region. The ground motion along this low-velocity channel is dominated by a Love wave packet with a dominant period near 4.5 sec. This guided wave is efficiently excited by both SE-NW rupture scenarios, but not appreciably by the NW-SE rupture scenario. The amplitudes are greater for SE-NW2 than for SE-NW1 because the former scenario has higher slip (and slip velocity) at the eastern end of the waveguide than does

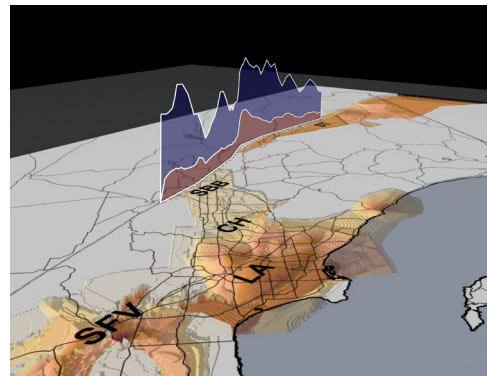


Figure 2. Source characteristics and crustal structure for the TeraShake simulations. Depth variation depict the isosurface of $V_s = 2.5$ km/s. Maximum slip (blue, <10.2 m) and maximum sliprate (red, <4.4 m/s) are projected along the TeraShake fault trace for the NW-SE and SE-NW1 rupture scenarios. CH = Chino Basin, LA = Los Angeles Basin, SBB = San Bernardino Basin, SBM = San Bernardino Mountains, SFV = San Fernando Valley, SGB = San Gabriel Basin, SGM = San Gabriel Mountains, and ST = Salton Trough. Other solid lines depict major freeways and the coastline.

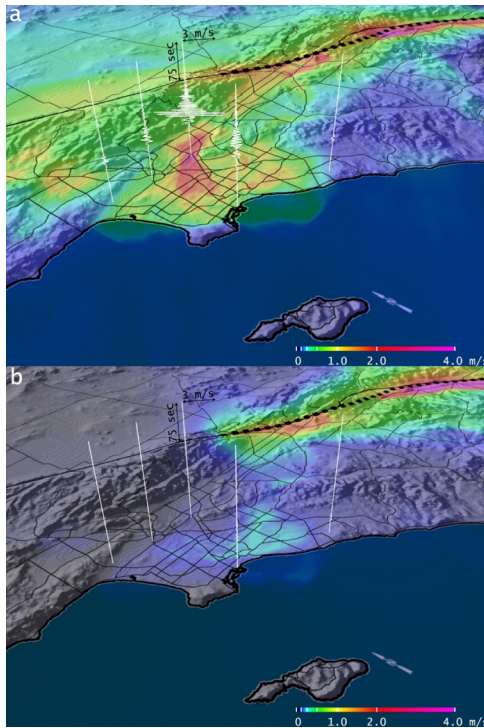


Figure 3. Maximum RMS PGV for the TeraShake ruptures. N50°W seismograms are superimposed at locations (from left to right) Westwood, downtown Los Angeles, Montebello, Long Beach, and Irvine. (a) SE-NW1 and (b) NW-SE scenarios.

the latter scenario, and therefore excites the guided wave even more effectively.

[9] Apart from the narrow strip of very high particle velocity immediately adjacent to the high-slip portions of the rupture, the highest ground motions occur in the San Gabriel and Los Angeles basins (Figure 4). There is an especially intense zone occurring near the transition between these basins (violet patch in each frame of Figure 4), a feature which is consistent between scenarios SE-NW1 and SE-NW2. Along the axis of the waveguide, the PGV exhibits a rapid local increase of more than a factor of 2 from all directions over distances as short as 10 km, leading to a sharp maximum where the sediment channel is narrowest (Figure 4). The local maximum occurs precisely where the sediment channel narrows, between the northwest end of the Puente Hills and the southern front of the San Gabriel Mountains (Whittier Narrows): the inset in Figure 4 shows the cross-sectional area of the sediment channel, as represented by the area inside the 2 km/s shear wave speed contour. The shape and amplitude of the local maximum can be understood surprisingly well by analogy with the response of a simple waveguide of varying cross-section. We consider a monochromatic mode propagating in a waveguide with slowly-varying (over distance of a wavelength) cross-section, and assume that the adiabatic approximation applies. In this approximation, the integral of energy flux over the cross-section is constant along the length of the waveguide. The squared particle velocity v^2 is proportional to the cross-section-averaged kinetic energy density, which is in turn

proportional to the ratio of cross-section-averaged energy flux to group velocity, and therefore

$$v \propto (CA)^{-1/2}, \quad (1)$$

where C is the group velocity and A is the cross-sectional area. In our case, the group velocity varies much less than the basin cross-section, and we would therefore expect amplitude modulation roughly of the form $v \sim A^{-1/2}$ to be associated with contraction of the sedimentary waveguide. As the inset in Figure 4 shows, the actual pattern of PGV follows precisely this shape near the ground motion maximum at Whittier-Narrows. Furthermore, analysis of the simulated seismograms shows a minimum of the dispersive Love wave group velocity in the area of the largest amplification, causing energy from a range of periods to arrive at almost the same time. Such phenomenon results in an Airy phase [Aki and Richards, 1980], which appears to be partly responsible for generating the large amplification.

[10] In contrast, the NW-SE scenario would generate PGV's of about an order of magnitude smaller in the Los Angeles basin, but strong reverberations for an extended duration at locations inside the Salton Trough, including the Coachella and Imperial Valleys. However, the Imperial Valley, especially south of the border, is a portion of the model that is poorly constrained by independent observations. Therefore, while we believe the prediction of strong trapping of energy and associated prolongation of high-amplitude long-period shaking is qualitatively correct, it is premature to cite quantitative predictions for PGV in this region.

[11] Both SE-NW and NW-SE rupture directions generate large ground motions near the rupturing fault segment, where the northern part of the Coachella Valley and the Palm Springs area feature the highest local seismic risk. The patterns of peak ground displacements (PGD's) inside the Los Angeles basin for the TeraShake simulations, sometimes used by engineers to predict building damage potential to very long-period structures such as highrises, are somewhat similar to those from the PGV's.

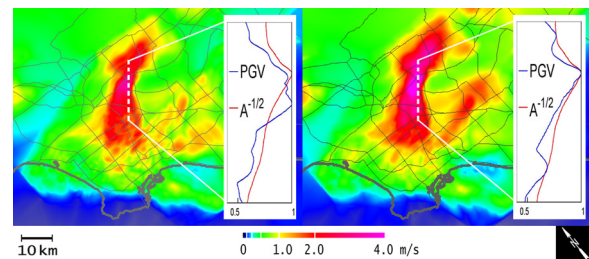


Figure 4. Maximum RMS PGV for (left) SE-NW1 and (right) SE-NW2 scenarios inside the black rectangle shown in Figure 1. The curves show the correlation of PGV (blue) and the reciprocal cross-sectional area ($A^{-1/2}$) of the sediment channel between the Los Angeles and San Gabriel basins, measured as the area of the vertical cross-section striking N50°W that lies inside the 2 km/s S-wave speed isosurface. Both curves are normalized to their respective maxima along the dashed profile. Lines on the maps depict major freeways and the coastline.

Fortunately, many locations of highrises, such as downtown Los Angeles, Long Beach, and Santa Monica/Westwood, prone to damage from such strong long-period ground motions, are located outside these areas of strong ground motion.

[12] The simulations used a fourth-order staggered grid finite-difference code [Olsen, 1994] with a coarse-grained implementation of the memory variables for a constant-Q solid [Day and Bradley, 2001], Q relations validated against data [Olsen et al., 2003], and Perfectly Matched Layers (PML) absorbing boundary conditions on the sides and bottom [Marcinkovich and Olsen, 2003]. The simulations required up to 19,000 CPU hours, using 240 processors (communicating via MPI) of the 10 teraflops IBM Power4+ DataStar supercomputer at San Diego Supercomputer Center (SDSC). Simulating four minutes of wave propagation took about 24 hours wall clock time for each scenario.

[13] These simulations demonstrate the critical role of the sedimentary waveguide along the southern border of the San Bernardino and San Gabriel Mountains in channeling seismic energy into the heavily populated San Gabriel and Los Angeles basin areas. The waveguide viewpoint provides a physical explanation for the predicted spatial pattern of ground motion in those basins, including the ground motion extremum where the two basins join. Less certain than the spatial pattern are the predicted absolute amplitudes of the ground motion extremes. Nonlinear soil effects were omitted in the TeraShake simulations, as they have ordinarily been considered unimportant at the relatively long periods modeled here [Yu et al., 1993]. However, nonlinearity induced by the higher-than-anticipated waveguide amplifications we have identified here would likely cause significant reduction of both shear modulus and Q factor in the near-surface layers. The resulting nonlinear losses during horizontal propagation through a confined sediment channel are not understood, previous work having focused on short-period, vertically-propagating body waves [Heuze et al., 2004], and this issue needs to be addressed in future simulations.

[14] **Acknowledgments.** The TeraShake Project is funded by NSF ITR through award EAR-0122464 (The SCEC Community Modeling Environment (SCEC/CME): An Information Infrastructure for System-Level Earthquake Research). SCEC is funded by NSF Cooperative Agreement EAR-0106924 and USGS Cooperative Agreement 02HQAG0008. SDSC's computational effort was supported through the NSF-funded SDSC Strategic Applications Collaborations (SAC) and Strategic Community Collaborations (SCC) programs. The large-scale computation, storage, visualization and access to scientific programming support were made possible by awards from the TeraGrid (TG-MCA03S012). The synthetic seismograms from TeraShake are available online at the Storage Resource Broker (SRB) at SDSC as well as animations of the simulated wave propagation (<http://www.scec.org/cme>). This is SCEC contribution 961.

References

- Aki, K., and P. G. Richards (1980), *Quantitative Seismology: Theory and Methods*, W. H. Freeman, New York.
- Bolt, B. A. (1968), The focus of the 1906 California earthquake, *Bull. Seismol. Soc. Am.*, *68*, 457–471.
- Day, S. M., and C. R. Bradley (2001), Memory-efficient simulation of anelastic wave propagation, *Bull. Seismol. Soc. Am.*, *91*, 520–531.
- Frankel, A. D., et al. (2002), Documentation for the 2002 update of the National Seismic Hazard maps, *U.S. Geol. Surv. Open File Rep. 02-420*.
- Graves, R. W. (1998), Three-dimensional finite-difference modeling of the San Andreas fault: Source parameterization and ground motion levels, *Bull. Seismol. Soc. Am.*, *88*, 881–897.
- Heuze, F., et al. (2004), Estimating site-specific earthquake ground motions, *Soil Dyn. Earthquake Eng.*, *24*, 199–233.
- Kohler, M., H. Magistrale, and R. Clayton (2003), Mantle heterogeneities and the SCEC three-dimensional seismic velocity model version 3, *Bull. Seismol. Soc. Am.*, *93*, 757–774.
- Magistrale, H., S. M. Day, R. W. Clayton, and R. W. Graves (2000), The SCEC southern California reference three-dimensional seismic velocity model version 2, *Bull. Seismol. Soc. Am.*, *90*, S65–S76.
- Marcinkovich, C., and K. Olsen (2003), On the implementation of perfectly matched layers in a three-dimensional fourth-order velocity-stress finite difference scheme, *J. Geophys. Res.*, *108*(B5), 2276, doi:10.1029/2002JB002235.
- Oglesby, D. D., D. S. Dreger, R. A. Harris, N. Ratchkovski, and R. Hansen (2004), Inverse kinematic and forward dynamic models of the 2002 Denali, Alaska earthquake, *Bull. Seismol. Soc. Am.*, *B6*, S214–S233.
- Olsen, K. B. (1994), Simulation of three-dimensional wave propagation in the Salt Lake basin, Ph.D. thesis, Univ. of Utah, Salt Lake City.
- Olsen, K. B., R. J. Archuleta, and J. Matarrese (1995), Three-dimensional simulation of a magnitude 7.75 earthquake on the San Andreas fault, *Science*, *270*, 1628–1632.
- Olsen, K. B., S. M. Day, and C. R. Bradley (2003), Estimation of Q for long-period (>2 s) waves in the Los Angeles basin, *Bull. Seismol. Soc. Am.*, *93*, 627–638.
- Pitarka, A., K. Irikura, T. Iwata, and H. Sekiguchi (1998), Three-dimensional simulation of the near-fault ground motion for the 1995 Hyogo-ken Nanbu (Kobe), Japan, earthquake, *Bull. Seismol. Soc. Am.*, *88*, 429–440.
- Sieh, K. (1978), Prehistoric large earthquakes produced by slip on the San Andreas fault at Palmett Creek, California, *J. Geophys. Res.*, *83*, 3907–3939.
- Sieh, K., and P. Williams (1990), Behavior of the southernmost San Andreas Fault during the past 300 years, *J. Geophys. Res.*, *95*, 6629–6645.
- Stüss, M. P., and J. H. Shaw (2003), P wave seismic velocity structure derived from sonic logs and industry reflection data in the Los Angeles basin, California, *J. Geophys. Res.*, *108*(B3), 2170, doi:10.1029/2001JB001628.
- Weldon, R., K. Scharer, T. Fumal, and G. Biasi (2004), Wrightwood and the earthquake cycle: What a long recurrence record tells us about how faults work, *Geol. Seismol. Am. Today*, *14*, 4–10.
- Working Group on California Earthquake Probabilities (1995), Seismic hazards in southern California: Probable earthquakes, 1994 to 2024, *Bull. Seismol. Soc. Am.*, *85*, 379–439.
- Yu, G., J. G. Anderson, and R. Siddharthan (1993), On the characteristics of nonlinear soil response, *Bull. Seismol. Soc. Am.*, *83*, 218–244.
- A. Chourasia, Y. Cui, M. Faerman, and R. Moore, San Diego Supercomputer Center, UCSD, 9500 Gilman Dr., La Jolla, CA 92093, USA.
- S. M. Day and K. B. Olsen, Department Geological Sciences, SDSU, 5500 Campanile Dr., San Diego, CA 92182, USA. (kbolsen@sciences.sdsu.edu)
- T. Jordan and P. Maechling, Department Earth Sciences, USC, Los Angeles, CA 90089, USA.
- J. B. Minster, Scripps Institution of Oceanography, UCSD, 9500 Gilman Dr., La Jolla, CA 92093, USA.